Science of the Total Environment 657 (2019) 498–508

Contents lists available at ScienceDirect

Science of the Total Environment

journal homepage: www.elsevier.com/locate/scitotenv

Prediction of CH_4 emissions from potential natural wetlands on the Tibetan Plateau during the 21st century

Tingting Li [a], Hailing Li [a], Qing Zhang [a,*], Zhenfeng Ma [b], Lingfei Yu [c], Yanyu Lu [d], Zhenguo Niu [e], Wenjuan Sun [c], Jia Liu [b]

[a] LAPC, Institute of Atmospheric Physics, Chinese Academy of Sciences, Beijing 100029, China
[b] Sichuan Climate Centre, Chengdu 610071, China
[c] State Key Laboratory of Vegetation and Environmental Change, Institute of Botany, Chinese Academy of Sciences, Beijing 100093, China
[d] Anhui Climate Center, Hefei 230031, China
[e] State Key Laboratory of Remote Sensing Science, Jointly Sponsored by Institute of Remote Sensing Applications, Chinese Academy of Sciences and Beijing Normal University, Beijing 100101, China

HIGHLIGHTS

- An integrated model framework based on $CH4MOD_{wetland}$, TOPMODEL and TEM was established.
- CH_4 fluxes will increase by 7.6%, 27.0% and 124.5% under CMIP5 scenarios by 2100.
- The dominant drivers for stimulating CH_4 fluxes are the temperature, precipitation and NPP.
- CH_4 fluxes showed decreasing trend from south to north, east to west.
- The potential natural wetlands on TP will emit 0.42–1.01 Tg CH_4 under CMIP5 scenarios by 2100.

GRAPHICAL ABSTRACT

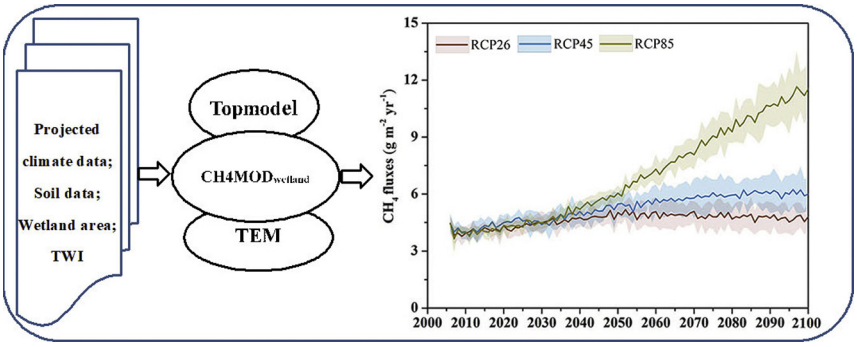

ARTICLE INFO

Article history:
Received 6 September 2018
Received in revised form 16 November 2018
Accepted 18 November 2018
Available online 28 November 2018

Editor: Sergi Sabater

Keywords:
CH_4 emissions
Tibetan plateau
Climate change
Model
Wetland

ABSTRACT

The alpine wetlands on the Tibetan Plateau (TP) are ecosystems vulnerable to global climate change. It has been recognized that future climate change may have a significant impact on methane (CH_4) emissions from the plateau, while less attention has been paid to predicting temporal and spatial variations in CH_4 emissions from TP natural wetlands. In this study, we used an integrated model framework based on the $CH4MOD_{wetland}$, TOPMODEL and TEM models to predict CH_4 emissions from potential natural wetlands on the TP under IPCC AR5 scenarios from 2006 to 2100. The model estimates suggest that the mean area-weighted CH_4 fluxes will increase from 4.45 ± 0.42 g m^{-2} yr^{-1} in 2006 to 4.79 ± 0.72, 5.99 ± 0.85 and 11.53 ± 1.33 g m^{-2} yr^{-1} under 3 Representative Concentration Pathway scenarios (RCP 2.6, RCP 4.5 and RCP 8.5 scenarios), respectively, by 2100. The dominant drivers stimulating CH_4 emissions are air temperature, precipitation and net primary productivity (NPP). Spatially, CH_4 fluxes and emissions showed a decreasing trend from south to north and from east to west. In response to climate change, a total of 0.42 ± 0.06, 0.54 ± 0.09 and 1.01 ± 0.12 Tg yr^{-1} of CH_4 emissions will be emitted from the TP's potential natural wetlands by the end of this century under the RCP 2.6, RCP 4.5 and RCP 8.5 scenarios, respectively.

1. Introduction

Methane (CH_4) is the most major long-lived anthropogenic greenhouse gas (GHG) after carbon dioxide (CO_2) (Myhre et al., 2013). CH_4

* Corresponding author.
E-mail address: zhangqing@mail.iap.ac.cn (Q. Zhang).

http://dx.doi.org/10.1016/j.scitotenv.2018.11.275
0048-9697/

has a global warming potential (GWP) of 28 over 100 years (Myhre et al., 2013) and contributed 17% of the direct anthropogenic radiative forcing in 2016 (Butler and Montzka, 2013). When the indirect global warming effects of CH_4 on aerosols and other chemical compounds (e.g., O3) are incorporated, CH_4 has a 10–40% larger current GWP (IPCC, 2013; Shindell et al., 2009).

Wetlands are the world's largest CH_4 source, with CH_4 emissions of 115 (Fung et al., 1991) to 270 Tg yr^{-1} (Melton et al., 2013), contributing approximately 20–25% of the total annual CH_4 emissions (Mitsch and Gosselink, 2007). CH_4 emissions from wetlands are the balance between CH_4 production (methanogenesis) and CH_4 oxidation (methanotrophy) (Bridgham et al., 2013). The main pathways of CH_4 emissions are through plants, ebullition, diffusion as well as hydrodynamic transport (Poindexter et al., 2016; Anthony and MacIntyre, 2016). These processes can be influenced by climatic factors such as temperature and precipitation. Temperature has a direct impact on methanogenesis and methanotrophy by affecting the activities and structures of microbial communities (Serrano-Silva et al., 2014; Whalen, 2005; Lew and Glińska-Lewczuk, 2018). Water table depth is a key factor that determines the anaerobic proportion of wetlands, where methanogenesis occurs (Bhullar et al., 2013; Ding et al., 2002; Moore and Roulet, 1993). Climate can directly influence the hydrological processes of a wetland by changing the input of precipitation (Hodson et al., 2011; Wei and Wang, 2017) and indirectly affect wetlands by changing evapotranspiration, near-surface permafrost and glacier and snow water equivalents (Yao et al., 2007; Zhang et al., 2011; Zhang et al., 2015). In addition, changes in temperature, precipitation, and other key environmental factors, coupled with increased CO_2 concentrations in the atmosphere, will influence plant species and productivity (Gao et al., 2016; Song et al., 2018) and further regulate methanogenic substrates and CH_4 transportation (Joabsson and Christensen, 2001; Joabsson et al., 1999; Li et al., 2016a; Walker et al., 2016).

The Tibetan Plateau (TP), located in southwest China, contains approximately one third of the wetland area in China (Niu et al., 2012) and contributes 30%–40% of the Chinese wetland soil organic matter (Zheng et al., 2013). As the 'third pole' of the earth (average elevation 4000 m a.s.l.) and one of the most fragile regions in the world, The TP is a "sensor" for global climate change (Schwalb et al., 2008). The climate changes in the TP are more significant than those in the rest of the northern hemisphere (Feng et al., 1998; Liu and Yin, 2002). During the past 5 decades, the TP has experienced significant warming and a slightly wetter climate (L. Li et al., 2010). The future projections based on the IPCC fifth phase of the Coupled Model Intercomparison Project5 (CMIP5) clearly indicate that the warming and wetting trend will continue on the Plateau over the 21st century (Zhang et al., 2015; Ji and Kang, 2013). The warmer and wetter climate will increase NPP (Zhuang et al., 2010) and supply more substrates for methanogens (Chen et al., 2013a). Meanwhile, permafrost thawing and glacier retreat might create larger or new freshwater marshes or lakes on the Plateau (Zhang et al., 2011). Chen et al. (2013b) reported that the TP contributes 63.5% of the CH_4 emissions from natural wetlands in China. The future climate will make the plateau a stronger CH_4 source, which should receive more attention from researchers and the government.

CH_4 observation experiments have been conducted and have shown high spatial and temporal variation in CH_4 fluxes from the wetlands on the TP (Chen et al., 2008; Hirota et al., 2004; Jin et al., 1999; Song et al., 2015; Wei et al., 2015). There have also been some studies estimating the CH_4 budget from natural wetlands on the TP using a book-keeping approach (Chen et al., 2013b; Ding et al., 2004; Jin et al., 1999) or process-based models (Jin et al., 2015; Li et al., 2016b; Wei and Wang, 2017). Compared with the book-keeping method, process-based models consider the impact of environmental conditions on CH_4 emissions and can reduce the uncertainties of regional estimations. We previously developed a biogeophysical model, $CH4MOD_{wetland}$, to simulate the processes of CH_4 production, oxidation and emission from natural wetlands (T. Li et al., 2010). The model is capable of capturing seasonal CH_4 variations and total annual CH_4 emissions from wetland sites in the Zoige and Haibei wetlands (Li et al., 2017) and has been applied for quantifying CH_4 emissions from wetlands on the TP for the past 60 years (Li et al., 2016b). The objective of this study is to use this model to project the temporal and spatial CH_4 emissions from natural wetlands on the TP during the 21st century under IPCC AR5 scenarios.

2. Materials and methods

2.1. Model framework

In a previous study, we utilized a model framework to estimate CH_4 emissions from natural wetlands on the TP from 1950 to 2010 (Li et al., 2016b). In this study, the same model framework (Fig. 1) was used to project the CH_4 emissions from 2006 to 2100 under the 3 Representative Concentration Pathway scenarios (RCP 2.6, RCP 4.5 and RCP 8.5

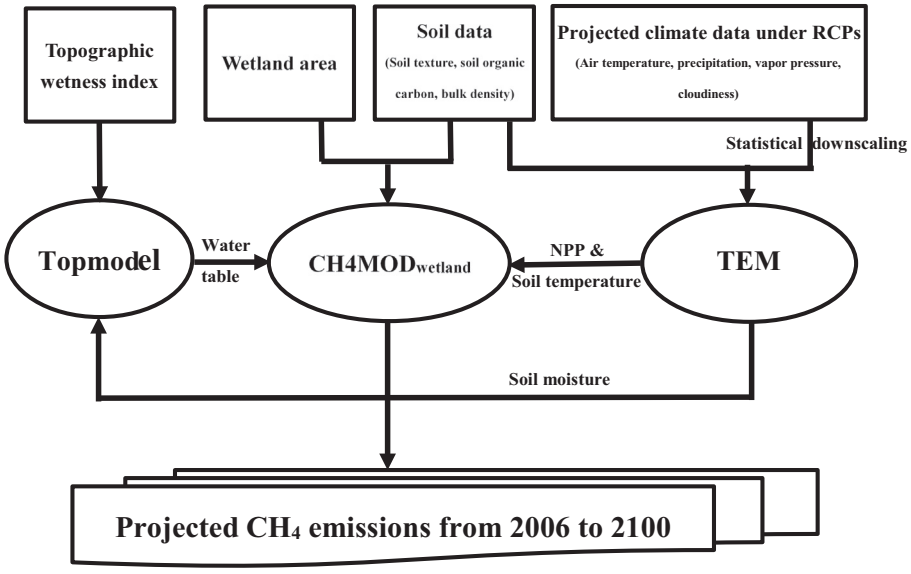

Fig. 1. Framework for projecting CH_4 emissions from potential natural wetlands on the TP between 2006 and 2100. $CH4MOD_{wetland}$ is a biogeophysical model to simulate CH_4 emissions from natural wetlands. TEM is a process-based biogeochemistry model that couples carbon, nitrogen, water, and heat processes in terrestrial ecosystems to simulate ecosystem carbon and nitrogen dynamics. TOPMODEL is a conceptual rainfall-runoff model that is designed to work at the scale of large watersheds using the statistics of topography.

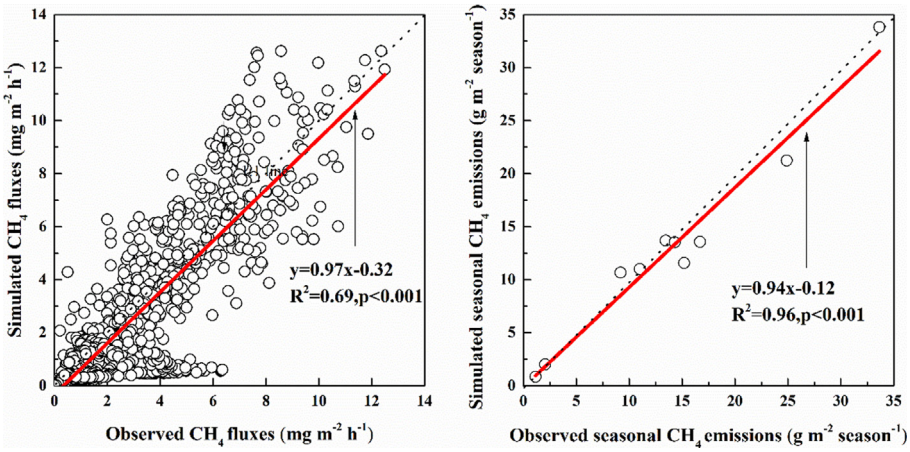

Fig. 2. Comparison of simulated with observed daily (a) and total seasonal (b) CH_4 fluxes from all of the sites on TP. Model correspondence (red solid line) is the regression line of simulated vs. observed CH_4 fluxes. The dashed line is a 1:1 line. (For interpretation of the references to color in this figure legend, the reader is referred to the web version of this article.)

scenarios). The model framework is based on 3 models: $CH4MOD_{wetland}$ (T. Li et al., 2010), TEM (Zhuang et al., 2004) and Topmodel (Beven and Kirkby, 1979) (Fig. 1).

$CH4MOD_{wetland}$ is the center of the model framework. This model is a biogeophysical, process-based model for simulating CH_4 fluxes and emissions from natural wetlands, including marshes, floodplains, peatland, and coastal wetlands. $CH4MOD_{wetland}$ was established based on CH4MOD, which is used to model CH_4 emissions from rice paddies (Huang et al., 1998a,b, 2004). According to the difference between the supply of methanogenic substrates from natural wetlands and rice paddies, $CH4MOD_{wetland}$ differs from CH4MOD by considering methanogenic substrates to be derived from root exudates, the decomposition of plant litter and soil organic matter (T. Li et al., 2010). CH_4 production is calculated by the availability of substrates and by soil environment influences, such as soil temperature, soil texture, redox potential and soil salinity. There are 3 means of CH_4 transportation, i.e., plant aerenchyma, ebullition and diffusion. When CH_4 is emitted via plant aerenchyma and diffusion, part of the CH_4 is oxidized. The inputs of the model include daily soil temperature, water table depth, the annual above-ground net primary productivity (ANPP), soil texture, soil organic matter, bulk density and wetland area. The outputs are the daily and annual CH_4 fluxes and emissions. More details about $CH4MOD_{wetland}$ have been well documented in previous studies (T. Li et al., 2010; Li et al., 2012, 2015, 2016b).

We integrated $CH4MOD_{wetland}$, TEM and Topmodel into a model framework (Fig. 1). TEM and Topmodel were used to supply the daily soil temperature, ANPP and daily water table depth to $CH4MOD_{wetland}$ (Fig. 1). TEM is a process-based ecosystem model that simulates the biogeochemical cycles of C and N between terrestrial ecosystems and the atmosphere (Zhuang et al., 2004, 2010). TEM has been widely used to estimate regional and global net primary productivity (Cramer et al., 1999; Jin et al., 2015; McGuire et al., 1992; Melillo et al., 1993). The TEM model is driven by projected climate data, including air temperature, precipitation, vapor pressure and cloudiness, and can simulate and output the soil temperature, soil moisture and ANPP, which can be the inputs of $CH4MOD_{wetland}$ and Topmodel (Fig. 1). Topmodel is a popular method to simulate regional water table depth in natural wetlands (Bohn et al., 2007; Kleinen et al., 2012; Lu and Zhuang, 2012; Zhang et al., 2017; Zhu et al., 2013). More details about the model framework have been described clearly in Li et al. (2016b).

2.2. Model calibration and validation

The main parameters that should be calibrated in $CH4MOD_{wetland}$ are vegetation index (*VI*), the fraction of CH_4 oxidized during plant mediated transport (P_{ox}) and the fraction of plant mediated transport available (T_{veg}). We calibrated these three parameters in previous studies (T. Li et al., 2010; Li et al., 2017) and keep the values in this study.

$CH4MOD_{wetland}$ has been validated in wetlands on the TP (Li et al., 2016b, 2017). In order to test the model performance prior to extrapolation to the TP, we validated the model against more observations of seasonal CH_4 variations at site scale. Table S1 describes the site information. Table S2 shows the parameters used in the simulation. We compared the seasonal variations of the observed and simulated CH_4 fluxes (Fig. S1). We also calculated some statistics to quantify the model performance. The statistics include the root mean square error (RMSE), the 95% RMSE, the mean deviation (RMD) and the model efficiency (EF). The details description and the equations to calculate these elements are described in Supplementary material S1.

The validation results show that although there were some discrepancies between the simulated and observed CH_4 fluxes, $CH4MOD_{wetland}$ can generally capture the seasonal variations at each site (Fig. S1, EF > 0 in Table 2). For example, at Haibei_2 site (Table S1), the model can't capture the peak CH_4 emissions during the soil thawing season (April to May) (Fig. S1e). The RMSE values indicate that although some simulated points lay outside the standard errors of the individual measured values, they fell within the 95% confidence interval for the whole dataset ($RMSE < RMSE_{95\%}$ in Table 2).

The model displayed a good performance in predicting the total seasonal CH_4 emissions (EF = 0.96 in Table 2). The regression of the computed versus observed total seasonal CH_4 emissions (Fig. 2b) resulted in an R^2 of 0.96, with a slope of 0.94 and an intercept of -0.12 gm^{-2} ($n = 10$, $p < 0.001$), which indicate that the differences of CH_4 emissions between sites and in different years can, in general, be simulated. A slight negative systematic bias existed between the simulated and observed seasonal CH_4 emissions (RMD = −6.8%).

2.3. Model extrapolation and data sources

Gridded (10 km × 10 km) and geo-referenced time-series input datasets of projected climate data, soil data, the topographic wetness

Table 1
Statistics of model performance on daily and seasonal CH_4 emissions from different sites.

Site	RMSE ($RMSE_{95\%}$) %	RMD %	EF	n
Zoige	53.8 (130.1)	−2.5	0.29	70
Namucuo	66.5 (318.2)	−14.6	0.84	27
Haibei_1	30.6 (61.0)	−5.4	0.05	12
Haibei_2	47.1 (133.8)	−13.9	0.53	841
Fenghuoshan	43.2 (276.5)	2.1	0.91	12
All (daily)	47.9 (140.4)	−12.8	0.56	962
All (season)	13.9 (126.6)	−6.8	0.96	10

Table 2
Information on the climate models.

Model name	Model center	Resolution	Reference
FGOALS-g2	LASG, Institute of Atmospheric Physic, Chinese Academy of Sciences, China	1.28° × 1.08°	Li et al. (2013)
HadGEM2-AO	Met Office Hadley Centre, United Kingdom	1.92° × 1.45°	Collins et al. (2008)
MIROC-ESM-LR	JAMSTEC, AORI, and NIES, Japan	1.28° × 0.64°	Watanabe et al. (2011)
MPI-ESM	Max Planck Institute for Meteorology, Hamburg, Germany	1.92° × 0.96°	Giorgetta et al. (2013)

index and wetland area (Table S3) were established to drive the model framework and make spatiotemporal estimates of CH_4 fluxes from the wetlands on the TP (Fig. 1).

The projected climate data from 2006–2100 under 3 RCPs (RCP2.6, RCP4.5 and RCP8.5) with four global climate models (GCMs) were used to drive the TEM model. RCP 2.6 is a pathway where radiative forcing peaks at approximately 3 W m^{-2} before 2100 and then declines to 2.6 W m^{-2} in 2100. The peak approximate CO_2 equivalent concentration reaches 490 ppm before 2100 under RCP 4.5, which comprises intermediate "stabilization pathways" in which radiative forcing is stabilized at approximately 4.5 W m^{-2} after 2100. RCP 8.5 is a "high pathway" in which radiative forcing reaches >8.5 W m^{-2} by 2100 and continues to rise for some amount of time. RCP 8.5 has an approximate CO_2 equivalent concentration of 1370 ppm in 2100. The four GCM models are FGOALS-g2, HadGEM2-AO, MIROC-ESM-LR and MPI-ESM. Table 1 shows the overview information of the four GCM models. The projected climate datasets were available from the Earth System Federation. However, the outputs of the GCMs have a coarser spatial resolution (Table 2); therefore, the projections were statistically downscaled to a resolution of 10 km × 10 km (Bertacchi Uvo et al., 2001; Lanza et al., 2001).

The soil texture data were used to assign texture-specific parameters to each grid cell in the TEM model, and the input parameters of $CH4MOD_{wetland}$ were derived from the soil map of the Food and Agriculture Organization of the United Nations (FAO/IIASA/ISRIC/ISS-CAS/JRC, 2012). The soil organic carbon content and the reference bulk density in wetland soils, which were the inputs of $CH4MOD_{wetland}$, were from the Harmonized World Soil Database (HWSD) (FAO/IIASA/ISRIC/ISS-CAS/JRC, 2008). The resolution of the soil datasets was 0.5° × 0.5° and was interpolated to 10 km × 10 km using the nearest neighbor approach. High-resolution global topographic index datasets were used to drive the TOPMODEL (Marthews et al., 2015).

Wetlands were defined in this study as land area that is permanently or seasonally saturated, excluding small ponds, lakes and rivers. During the past 60 years, wetland lost significantly on TP due to global warming as well as draining and reclamation of the land as farmland (Niu et al., 2012). The estimated wetland area in 2008 from TP was only 33,400 km^2 in 2008 (Niu et al., 2012). After joining the Ramsar Convention in 1992, the Chinese government has increasingly recognized the importance of wetland protection (Wang et al., 2012). In this study, we assumed that without human influences, the wetlands on TP would develop to its potential status in future. The potential distribution of wetlands is defined as the spatial distribution of wetlands that would exist if there were no human activities on earth (Hu et al., 2017). Hu et al. (2015, 2017) simulated the potential distribution of global wetlands by employing a new Precipitation Topographic Wetness Index (PTWI) and global remote sensing training samples. We extracted the potential wetland distribution on TP from this dataset (Fig. 3). The potential wetland area excluding small ponds, lakes and rivers is 88,500 km^2 on the TP, much higher than the present wetland area on TP.

A total of 12 simulations (3 scenarios × 4 GCM datasets) were processed in this study. The model framework was run in each grid for the grid level of CH_4 fluxes and emissions. The area-weighted average CH_4 fluxes on the whole TP wetland area were based on the potential natural

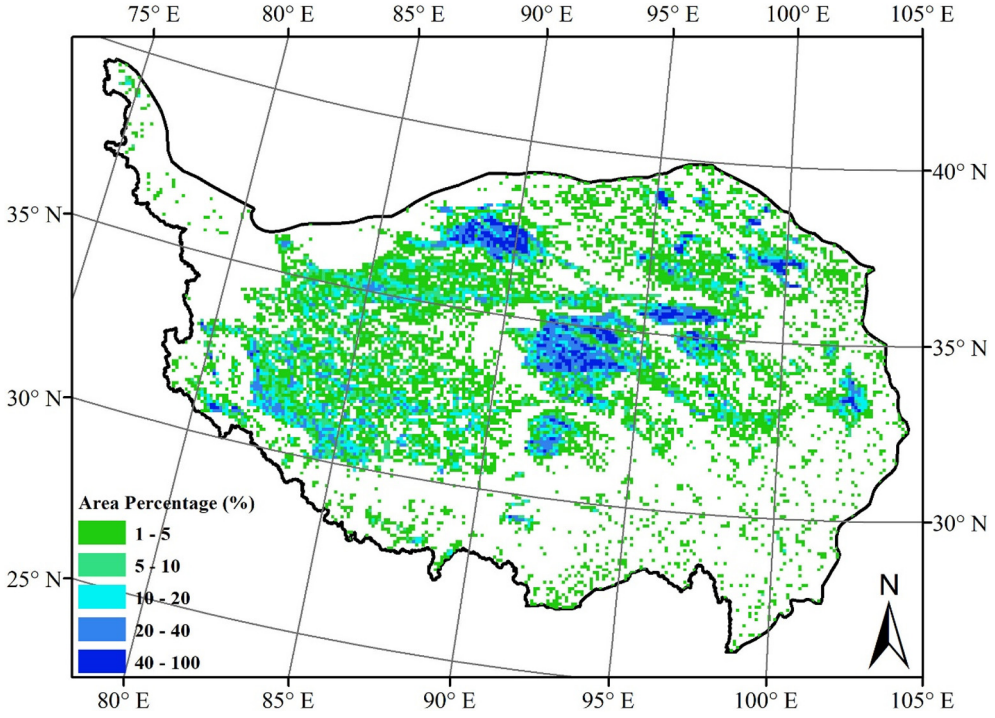

Fig. 3. Potential natural wetland distribution on the TP. The area percentage represents the percentage of the total area of the grid (100 km^2) that is wetland area. Data are extracted from the global potential wetland distribution by Hu et al. (2017).

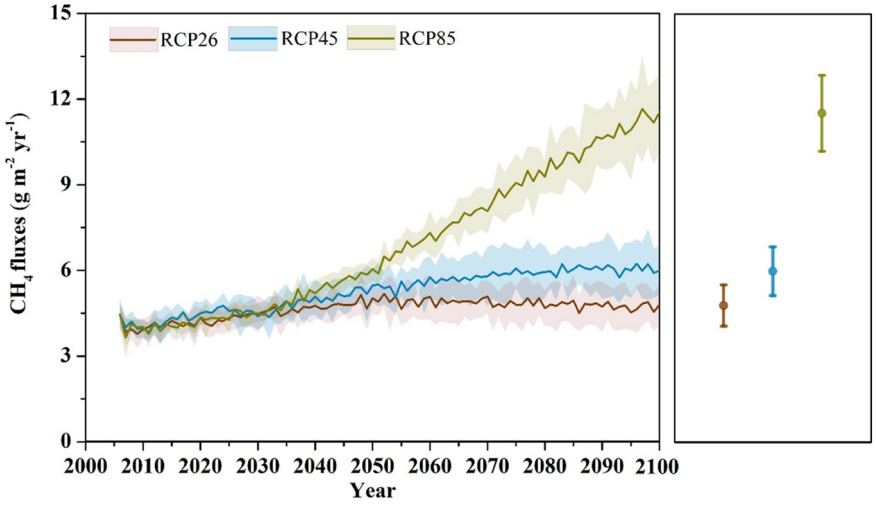

Fig. 4. Projected CH_4 fluxes in RCP 2.6, RCP 4.5 and RCP 8.5. Colored solid lines represent ensemble average simulations by GCM climate models, and the shaded areas around each line represent one standard deviation. (For interpretation of the references to color in this figure legend, the reader is referred to the web version of this article.)

wetland distribution. The total CH_4 emissions from the potential natural wetlands on the TP were the sum of the CH_4 emissions from each grid.

3. Results and discussion

3.1. Projected temporal trends in CH_4 emissions from potential natural wetlands on the TP

Mean area-weighted CH_4 fluxes from the potential natural wetlands on the TP were projected to increase from 4.45 ± 0.42 g m^{-2} yr^{-1} in 2006 to 4.79 ± 0.72, 5.99 ± 0.85 and 11.53 ± 1.33 g m^{-2} yr^{-1} under RCP 2.6, RCP 4.5 and RCP 8.5, respectively, by 2100 (Fig. 4). The regional annual CH_4 fluxes showed a significant increase from 2006 to 2100, with a rate of 0.09 g m^{-2} per decade (R^2 = 0.49, $p < 0.001$), 0.24 g m^{-2} per decade ($R^2 = 0.93$, $p < 0.001$), and 0.88 g m^{-2} per decade ($R^2 = 0.96$, $p < 0.001$) in RCP 2.6, RCP 4.5 and RCP 8.5, respectively.

In RCP 2.6, the mean area-weighted annual CH_4 fluxes reached a maximum value of 4.95 ± 0.62 g m^{-2} yr^{-1} and then declined (Table 3). In contrast, annual mean CH_4 fluxes were projected to increase to the peak of 6.04 ± 0.78 g m^{-2} yr^{-1} in the 2080s and remain constant thereafter in RCP 4.5 (Table 3). In RCP 8.5, the mean area-weighted annual CH_4 fluxes were projected to increase throughout the century. The projected mean annual CH_4 flux was 2.75 times larger in the 2090s than in the beginning of the century (Table 3).

The estimated wetland area from remote sensing data was 33,400 km^2 in 2008 (Niu et al., 2012). The potential wetland area is projected to be 88,500 km^2 (Hu et al., 2015, 2017). If the area of the natural wetlands on the TP reaches the potential wetland distribution by 2050, the entire TP wetlands will emit 0.43 ± 0.05, 0.47 ± 0.06 and 0.52 ± 0.03 Tg CH_4 yr^{-1} in 2050 under RCP 2.6, RCP 4.5 and RCP 8.5, respectively (Table 4). However, if natural wetlands reach the potential wetland distribution by the end of this century, a total of 0.42 ± 0.06, 0.54 ± 0.09 and 1.01 ± 0.12 Tg yr^{-1} of CH_4 emissions will be emitted in 2100 from the natural wetlands of the TP (Table 4). If we assume that the wetland area will expand linearly from 2008 to 2100, the cumulative CH_4 emissions from the natural wetlands will be 38.27 ± 4.75, 43.50 ± 5.59 and 57.54 ± 5.12 Tg yr^{-1} under RCP 2.6, RCP 4.5 and RCP 8.5 from 2008 to 2100, respectively.

Table 3
Decadal variations in CH_4 fluxes under CMIP5 scenarios.

Decades	CH_4 fluxes (g m^{-2} yr^{-1})		
	RCP 2.6	RCP 4.5	RCP 8.5
2006–2010	3.98 ± 0.39	4.12 ± 0.38	4.05 ± 0.35
2010–2020	4.07 ± 0.38	4.19 ± 0.40	4.02 ± 0.32
2021–2030	4.32 ± 0.46	4.57 ± 0.45	4.41 ± 0.34
2031–2040	4.61 ± 0.47	4.77 ± 0.58	4.90 ± 0.36
2041–2050	4.81 ± 0.51	5.17 ± 0.63	5.69 ± 0.38
2051–2060	4.95 ± 0.62	5.47 ± 0.66	6.72 ± 0.46
2061–2070	4.91 ± 0.66	5.70 ± 0.79	7.75 ± 0.62
2071–2080	4.83 ± 0.69	5.91 ± 0.95	9.01 ± 0.86
2081–2090	4.79 ± 0.75	6.04 ± 0.78	10.11 ± 1.08
2091–2100	4.72 ± 0.71	6.04 ± 0.97	11.12 ± 1.30

3.2. Projected spatial variation in CH_4 emissions from potential natural wetlands on the TP

Fig. 5a shows the spatial distribution of mean CH_4 fluxes under RCP 2.6, RCP 4.5 and RCP 8.5 from 2006 to 2010. From south to north and east to west, CH_4 fluxes decreased. Higher CH_4 fluxes occurred in the northeastern, eastern and southeastern edges of the TP, where the altitude was almost under 4000 m (Wei et al., 2015). The eastern edge of the Plateau, where the Zoige wetland is located, showed peak fluxes as high as 40 g m^{-2} yr^{-1} (Fig. 5a). The spatial patterns were similar at the end of 21st century under different CMIP5 RCP scenarios. Over the century CH_4 fluxes were projected to increase in most of the wetlands on the TP, with different increments between different wetlands and RCPs scenarios (Fig. 5b, c and d). The projected increases in CH_4 fluxes showed similar spatial patterns under RCP 2.6, RCP 4.5 and RCP 8.5 and were higher in the southeast and lower in the northwest (Fig. 5b, c and d). In RCP 2.6, CH_4 fluxes were projected to increase by 0–5 g m^{-2} yr^{-1} from most of the wetlands, except for wetlands of the southeastern edge of the TP, which demonstrated an increment of approximately 5–10 g m^{-2} yr^{-1} (Fig. 5b). In RCP 4.5, the increment of CH_4 fluxes reached 10–20 g m^{-2} yr^{-1} in the southeastern region of

Table 4
List of $CH4MOD_{wetland}$ simulated wetland CH_4 emissions for future RCPs by CMIP5 models.

Model	CH_4 emissions by 2050 (Tg CH_4 yr^{-1})			CH_4 emissions by 2100 (Tg CH_4 yr^{-1})		
	RCP 2.6	RCP 4.5	RCP 8.5	RCP 2.6	RCP 4.5	RCP 8.5
FGOALS-g2	0.38	0.40	0.49	0.37	0.44	0.93
HadGEM2-AO	0.47	0.52	0.54	0.45	0.61	1.02
MIROC-ESM-LR	0.48	0.51	0.55	0.49	0.61	1.16
MPI-ESM	0.41	0.45	0.49	0.37	0.49	0.92
MEAN ± Sd	0.43 ± 0.05	0.47 ± 0.06	0.52 ± 0.03	0.42 ± 0.06	0.54 ± 0.09	1.01 ± 0.12

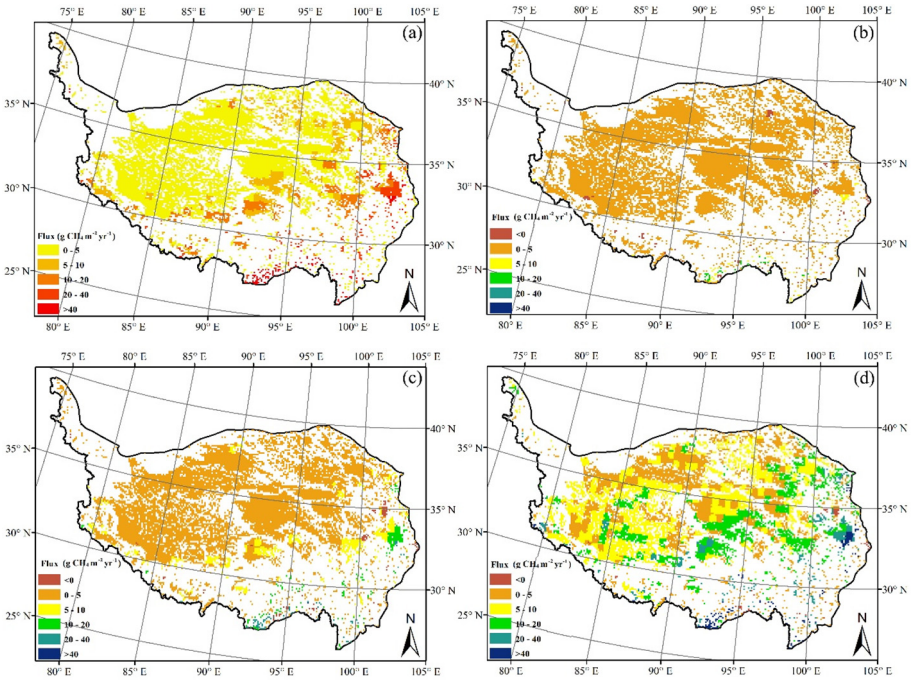

Fig. 5. Spatial variations of CH_4 fluxes. (a) Mean CH_4 fluxes under the CMIP5 RCPs from 2006 to 2010; (b) mean CH_4 fluxes under RCP 2.6 in the 2090s minus mean CH_4 fluxes under the CMIP5 RCPs from 2006 to 2010; (c) mean CH_4 fluxes under RCP 4.5 in the 2090s minus mean CH_4 fluxes under the CMIP5 RCPs from 2006 to 2010; (d) mean CH_4 fluxes under RCP 8.5 in the 2090s minus mean CH_4 fluxes under the CMIP5 RCPs from 2006 to 2010.

the TP (Fig. 5c). The projected CH_4 fluxes roughly doubled in most of the wetlands by the 2090s in RCP 8.5 (Fig. 5d).

The spatial patterns of the grid-level regional CH_4 emissions were similar to those of the CH_4 fluxes (Figs. 5a and 6a). The intense CH_4 source regions are located at the eastern edge and in the central TP, with CH_4 emissions higher than 800 t CH_4 yr^{-1} from 2006 to 2100 in the CMIP5 RCP scenarios (Fig. 6a). The highest CH_4 increment also occurred in these two regions, with values of 50–100 t under RCP 2.6 (Fig. 6b), 100–200 t under RCP 4.5 (Fig. 6c) and >200 t under RCP 8.5 (Fig. 6d).

Based on previous observations, CH_4 fluxes show strong spatial heterogeneity across the natural wetlands on the TP. These differences may be due to soil temperature, soil moisture, soil organic carbon, altitude and plant biomass (Wei et al., 2015). Our simulations were similar to previous observations. For example, previous studies have shown

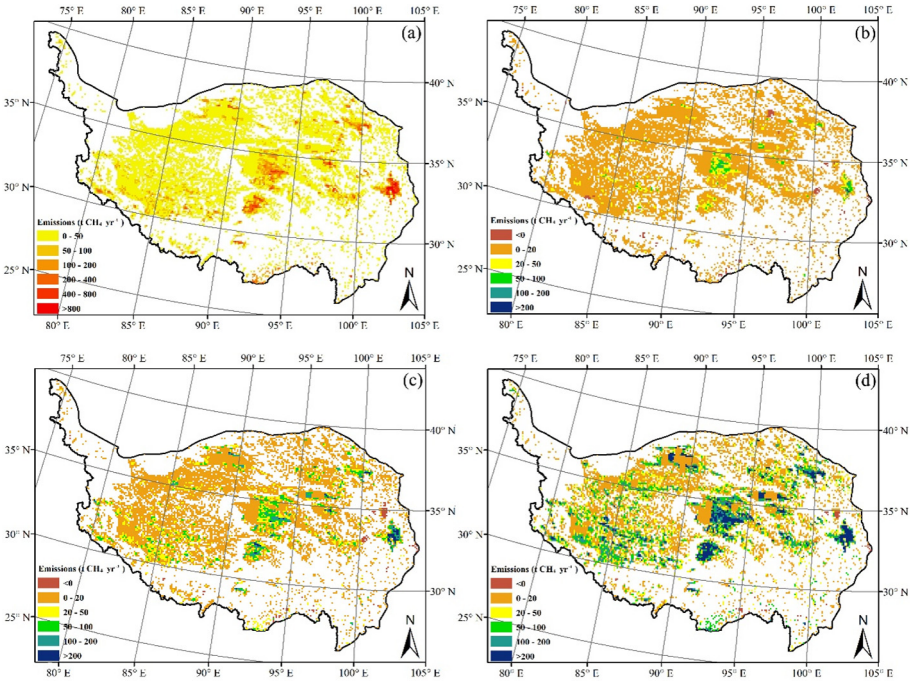

Fig. 6. Spatial variations of regional CH_4 emissions. (a) Mean CH_4 emissions under the CMIP5 RCPs from 2006 to 2010; (b) mean CH_4 emissions under RCP 2.6 in the 2090s minus mean CH_4 emissions under the CMIP5 RCPs from 2006 to 2010; (c) mean CH_4 emissions under RCP 4.5 in the 2090s minus mean CH_4 emissions under the CMIP5 RCPs from 2006 to 2010; (d) mean CH_4 emissions under RCP 8.5 in the 2090s minus mean CH_4 emissions under the CMIP5 RCPs from 2006 to 2010.

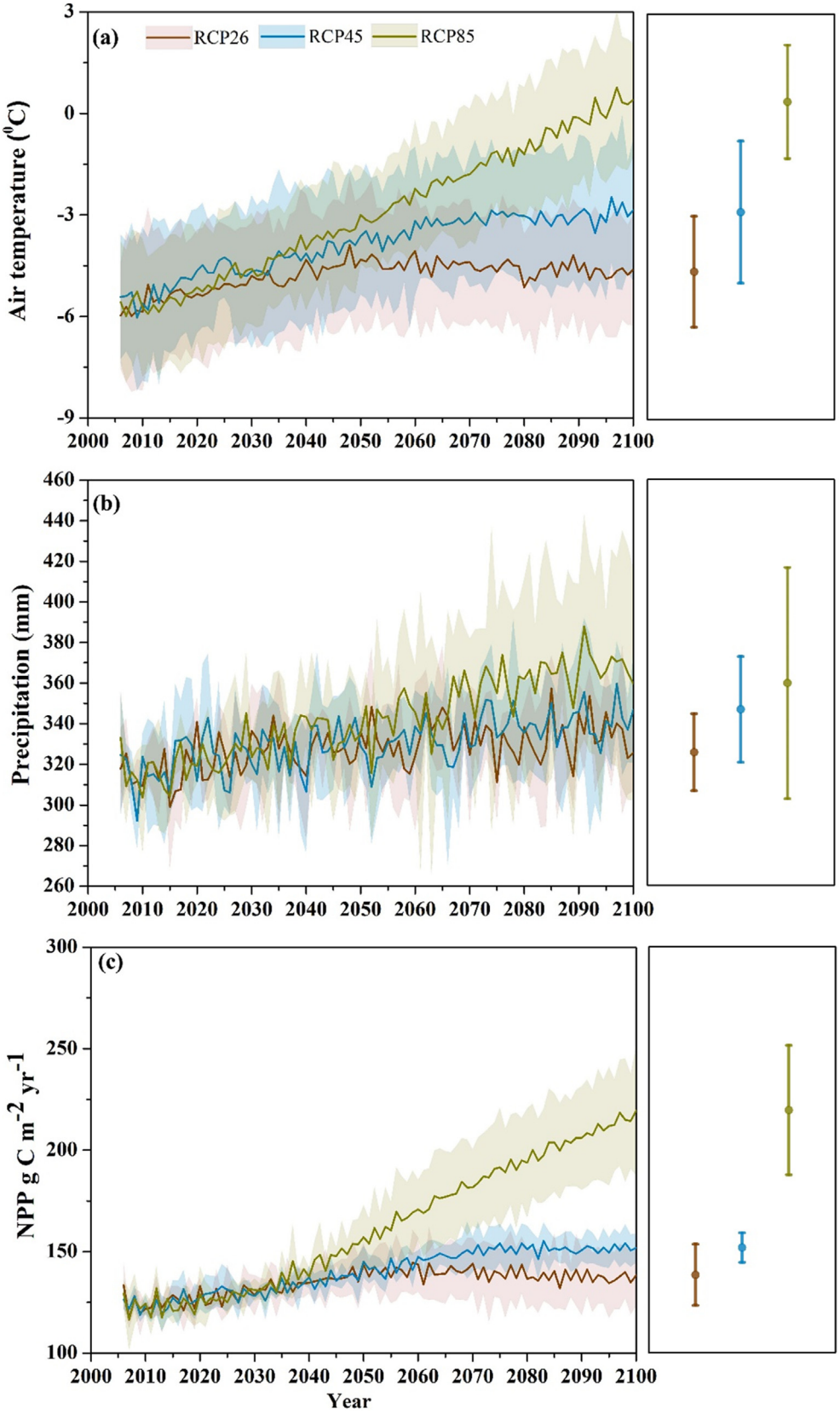

Fig. 7. Projected temporal trends of air temperature (a) and precipitation (b) by climate models and NPP (c) by TEM. The colored solid lines represent ensemble average simulations outputted by the GCM climate models or from using GCM climate models, and the shaded areas around the lines represent one standard deviation. (For interpretation of the references to color in this figure legend, the reader is referred to the web version of this article.)

higher CH_4 fluxes in the Zoige wetlands than in other places on the TP, with values of 11–56 g m^{-2} yr^{-1} (Chen et al., 2008; Ding et al., 2004; Wang et al., 2002). The simulated CH_4 fluxes were approximately 20–40 g m^{-2} yr^{-1} in Zoige regions and were higher than those in other regions on the TP (Fig. 5a). At Huashixia, Nam Co and Haibei, the observed CH_4 fluxes were 5.3–6.7 g m^{-2} yr^{-1} (Jin et al., 1999), 0.6 g m^{-2} yr^{-1} (Wei et al., 2015) and 11.1–33.8 g m^{-2} yr^{-1} (Hirota et al., 2004; Song et al., 2015), respectively. The simulated CH_4 fluxes were also comparable to the observed fluxes, with values of 5–10, 0–5 and 10–20 g m^{-2} yr^{-1} (Fig. 5a).

Previous modeling studies on the TP have shown similar distributions of CH_4 fluxes. Most of the simulations, e.g., Wei and Wang (2017), Jin et al. (2015) and Xu and Tian (2012), show the highest CH_4 emissions from the eastern region of the TP. Liu et al. (2015) also modeled a decrease in CH_4 emissions from the southeast to northwest. Jin's simulations (Jin et al., 2015) show higher CH_4 fluxes in the eastern, northeastern and central regions of the TP, which is similar to our simulations (Fig. 5a).

3.3. Impact of environmental drivers on CH_4 emissions

The temporal variation in CH_4 fluxes was strongly influenced by the air temperature, precipitation and NPP (Fig. 8). The area-weighted annual mean air temperature, annual precipitation and annual NPP showed a significant increase from 2006 to 2100 ($p < 0.001$) (Fig. 7), which promotes CH_4 emissions (Fig. 4). Under RCP 2.6, the maximum air temperature and NPP were found during the 2050s, and the maximum annual precipitation was found in the 2060s, and then declined thereafter (Fig. 7). This corresponded to the temporal CH_4 variations (Table 3, Fig. 4). An increase of almost 50% (Fig. 4, Table 3) in CH_4 fluxes was promoted by the increases in air temperature, precipitation and NPP under RCP 4.5 (Fig. 7). Under RCP 8.5, an increase of 5.8 °C in air temperature, an 18% increase in precipitation and a 72% increase in NPP resulted in an increase of 175% in CH_4 fluxes (Table 3). Significant positive correlations were found between the annual mean CH_4 flux and temperature (Fig. 8a, b and c), the CH_4 flux and annual precipitation (Fig. 8d, e and f), and the CH_4 flux and annual NPP (Fig. 8g, h and i). This result suggested that warmer, wetter climates and CO_2 fertilization will accelerate CH_4 emissions from the wetlands on the TP during the 21st century.

Global climate change is likely to stimulate CH_4 emissions from natural wetlands (Dean et al., 2018; Erwin, 2009; Yvon-Durocher et al., 2014). Temperature can stimulate methanogenic activity and CH_4 oxidation (Frenzel and Karofeld, 2000; Kip et al., 2010; van Winden et al., 2012), but CH_4 oxidation rates are less temperature dependent than CH_4 production (Schipper et al., 2014). A rise in precipitation can enhance the water table depth, extend the wetland area and increase the rate of organic substrate leaching to deeper parts of the peat profile, which can induce higher CH_4 production. The historic CH_4 fluxes from wetlands across the TP were significantly and positively correlated with air temperature and precipitation (Li et al., 2016b; Zhu et al., 2016). The simulated results of this study show that these relationships will continue in the 21st century (Fig. 6a and b). Temperature and precipitation were also found to be the most important controlling factors for CH_4 emissions in northeastern China over the past 3 decades (Wei and Wang, 2016; Zhu et al., 2016) as well as in the 21st century (Li et al., 2016c). In addition, several modeling studies have documented the positive effects of warmer temperatures and CO_2 fertilization on NPP (Jin et al., 2015; Li et al., 2016c; Melillo et al., 1993; Wieder et al., 2015; Zhou et al., 2018), which can supply more methanogenic substrates and promote CH_4 production (King and Reeburgh, 2002; Whiting and Chanton, 1993). These results are also consistent with our analysis (Figs. 7c, 8g, h and i).

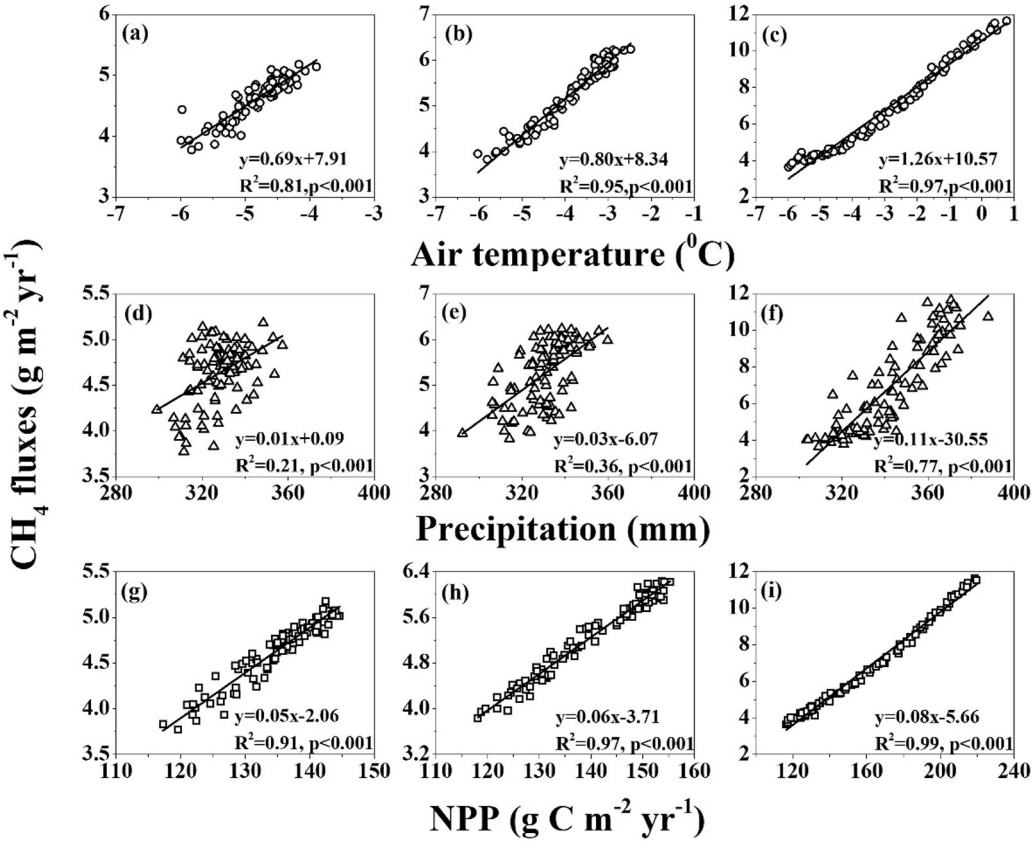

Fig. 8. Regression between annual mean CH_4 fluxes and air temperature in RCP 2.6 (a), RCP 4.5 (b), RCP 8.5 (c); regression between annual mean CH_4 fluxes and annual precipitation in RCP 2.6 (d), RCP 4.5 (e), RCP 8.5 (f); regression between annual mean CH_4 fluxes and annual NPP in RCP 2.6 (g), RCP 4.5 (h), RCP 8.5 (i).

3.4. Uncertainties and future needs

This study projected CH_4 emissions from natural wetlands under the RCP 2.6, RCP 4.5 and RCP 8.5 scenarios during the 21st century. Comparing with previous modeling studies, there are large uncertainties in predicting CH_4 fluxes under different climate conditions in different regions. Jin et al. (2015) predicted CH_4 increases of 1.2, 2.3 and 5.3 g m^{-2} yr^{-1} under the RCP 2.6, RCP 4.5 and RCP 8.5 scenarios in natural wetlands on the TP by 2100. Our results are lower than Jin's results under RCP 2.6 (0.9 g m^{-2} yr^{-1}) and RCP 4.5 (1.9 g m^{-2} yr^{-1}) and are higher than Jin's result under RCP 8.5 (7.1 g m^{-2} yr^{-1}) (Fig. 4 and Table 3). Under the RCP 2.6 scenario, most previous modeling studies, e.g., Jin's prediction for the TP (Jin et al., 2015), Zhang's prediction for global natural wetlands (Zhang et al., 2017) and our previous study for the Sanjiang Plain (Li et al., 2016c), predicted a peak CH_4 flux in 2050 followed by a decreasing trend in CH_4 emissions. Liu et al. (2015) predicted that the peak CH_4 flux from Chinese natural wetlands would appear in 2075 under RCP 2.6. The predicted increases in CH_4 fluxes range from 30% to 78% under the RCP 4.5 scenario (Jin et al., 2015; Li et al., 2016c; Liu et al., 2015; Zhang et al., 2017) or the doubled CO_2 scenario (Shindell et al., 2004). For the RCP 8.5 scenario, our results show a greater increase in CH_4 emissions than Jin's results for wetlands on the TP (Jin et al., 2015), Liu's results for Chinese wetlands (Liu et al., 2015) and Zhang's results for global wetlands (Zhang et al., 2017). However, our results are consistent with Zhuang's results (Zhuang et al., 2006), which predict that CH_4 emissions from wetlands in northern high latitudes will more than double over the century in a scenario with a projected atmospheric CO_2 mole fraction of approximately 1152 ppm by 2100.

In this study, the uncertain in projecting CH_4 emissions is due to several factors. Insufficient model processes represent the first factor that may induce uncertainty in future projections. The present model lacks some physical and biogeochemical processes that induce uncertainties in model simulations. For example, warming-induced permafrost thawing would result in substantial emissions of old CH_4 on the TP (Chen et al., 2013a). However, this process is not described in the present model. Another example is the effect of nitrogen deposition, which can regulate plant growth, methanogenesis and methanotrophy (Gomez-Casanovas et al., 2016; Liu and Greaver, 2009) and should also be considered in the present model. Poindexter et al. (2016) reported that most of the previous models overlooked the hydrodynamic transport. How emissions are partitioned among the transportation ways in large-scale regional and global models of wetland CH_4 emissions should be reassessed in future (Anthony and MacIntyre, 2016). If possible, more detailed physical and biogeophysical processes with sufficient data support are necessary in future model development.

The second factor that results in uncertainties in CH_4 projections are vegetation impacts. Future climate change can change both NPP and the distribution of vegetation across the TP (Gao et al., 2016; Song et al., 2018). The simulation results by Gao et al. (2016) show that the area of forests and shrubs will increase and the area of alpine meadows will decrease under future climate conditions. Vegetation contributes significantly to methanogenic substrates (Minoda et al., 1996; Whiting and Chanton, 1992) and methanogenic community composition (Cui et al., 2015). Different plant species have different substrate qualities, above- and belowground production dynamics, rhizosphere effects, and plant-mediated transport (Berrittella and Huissteden, 2011; Bhullar et al., 2013; Dorodnikov et al., 2011; Li et al., 2016a; Ström et al., 2005). In this study, we assumed that the vegetation distribution will not change in the future, which may induce a large uncertainty in the CH_4 simulation. In the future, changes in the vegetation distribution should be considered in the simulation. In addition, more calibration and validation according to different vegetation communities should be made to improve predictions of CH_4 emissions (Bridgham et al., 2013).

Last but not least, poor projections of the wetland extent inevitably induce large uncertainties in simulations of future regional CH_4 emissions. The estimated wetland area of natural wetlands on the TP during the 1990s and 2000s ranged from 32,000 km^2 to 188,000 km^2, which induced estimated regional CH_4 emissions of 0.06 to 1.25 Tg from the present wetlands on the TP (Chen et al., 2013a; Ding et al., 2004; Jin et al., 1999; Jin et al., 2015; Li et al., 2016b; Wei et al., 2015; Xu and Tian, 2012; Zhang and Jiang, 2014). Jin et al. (2015) used the wetland distribution from Papa et al. (2010) of 134,000 km^2 and projected CH_4 emissions of 1.13, 1.42 and 1.68 Tg yr^{-1} in the 2090s under the RCP 2.6, RCP 4.5 and RCP 8.5 scenarios, respectively. We used an area of 88,500 and projected totals of 0.42, 0.54 and 1.01 Tg CH_4 yr^{-1} in 2050 under the same scenarios in 2100 (Table 3). Different wetland distributions resulting from different methods (Zhang et al., 2016) induce large uncertainties in estimated regional CH_4 emissions. Future wetland projections should depend on both climate change and human activities (Erwin, 2009). Alpine wetland ecosystems are severely impacted by climate change due to their fragmentation (Xue et al., 2014). Precipitation will be the main driver of the growth of freshwater marshes in the TP in the future (Xue et al., 2014). Warmer temperatures will cause the Plateau to be drier in the future. However, these warmer temperatures may also cause frozen areas to thaw and glaciers to melt (Zhao et al., 2004). Wetland restoration was planned by the China National Wetland Conservation Action Plan (NWCP) (Editorial Committee, 2009). However, climate change will make wetland restoration more complex (Erwin, 2009). Considering the difficulties and uncertainties in predicting the wetland extent in the TP, we used the potential natural wetland to represent the future wetland distribution on the TP (Hu et al., 2017). In the future, more attention should be paid to predicting wetland extent to reduce the uncertainties in estimating regional CH_4 emissions.

4. Conclusions

This study projected temporal and spatial vitiations of CH_4 emissions from potential natural wetlands across the TP from 2006 to 2100 using an integrated model framework based on $CH4MOD_{wetland}$, TEM and Topmodel. The model simulation shows that the average CH_4 fluxes will increase by 7.6%, 27.0% and 124.5% under the RCP 2.6, RCP 4.5 and RCP 8.5 scenarios, respectively, by 2100. The dominant drivers of the increases in CH_4 fluxes are air temperature, precipitation and NPP. The total CH_4 emissions will reach 0.42 ± 0.06, 0.54 ± 0.09 and 1.01 ± 0.12 Tg yr^{-1} under the RCP 2.6, RCP 4.5 and RCP 8.5 scenarios, respectively, if the natural wetland reaches a potential wetland area of 88,500 km^2 by the end of this century. At a regional scale, higher CH_4 fluxes will occur in the northeastern, eastern and southeastern edges of the TP. To reduce the uncertainties in predictions of regional CH_4 emissions from the TP, more attention should be paid to model improvement and the acquisition of more reliable information on wetland and vegetation distributions in the future.

Acknowledgments

This work was supported by the National Natural Science Foundation of China (Grant No. 41775159, 31670484 and 31000234) and the Climate Change Special Foundation of China Meteorological Administration (CCSF201823).

Appendix A. Supplementary data

Supplementary data to this article can be found online at https://doi.org/10.1016/j.scitotenv.2018.11.275.

References

Anthony, K.W., MacIntyre, S., 2016. Biogeochemistry: nocturnal escape route for marsh gas. Nature 535, 363–365.

Berrittella, C., Huissteden, J., 2011. Uncertainties in modelling CH_4 emissions from northern wetlands in glacial climates: the role of vegetation parameters. Clim. Past 7, 1075–1087.

Bertacchi Uvo, C., Olsson, J., Morita, O., Jinno, K., Kawamura, A., Nishiyama, K., et al., 2001. Statistical atmospheric downscaling for rainfall estimation in Kyushu Island, Japan. Hydrol. Earth Syst. Sci. 5, 259–271.

Beven, K., Kirkby, M.J., 1979. A physically based, variable contributing area model of basin hydrology. Hydrol. Sci. Bull. 24, 43–69.

Bhullar, G.S., Iravani, M., Edwards, P.J., Venterink, H.O., 2013. Methane transport and emissions from soil as affected by water table and vascular plants. BMC Ecol. 13, 32.

Bohn, T., Lettenmaier, D., Sathulur, K., Bowling, L., Podest, E., McDonald, K., et al., 2007. Methane emissions from western Siberian wetlands: heterogeneity and sensitivity to climate change. Environ. Res. Lett. 2, 045015.

Bridgham, S.D., Cadillo-Quiroz, H., Keller, J.K., Zhuang, Q., 2013. Methane emissions from wetlands: biogeochemical, microbial, and modeling perspectives from local to global scales. Glob. Chang. Biol. 19, 1325–1346.

Butler, J.H., Montzka, S.A., 2013. The NOAA Annual Greenhouse Gas Index (AGGI). National Oceanic and Atmospheric Administration (NOAA).

Chen, H., Yao, S., Wu, N., Wang, Y., Luo, P., Tian, J., et al., 2008. Determinants influencing seasonal variations of methane emissions from alpine wetlands in Zoige Plateau and their implications. J. Geophys. Res.-Atmos. 113, D12303. https://doi.org/10.1029/2006JD008072 (1984–2012).

Chen, H., Zhu, Q., Peng, C., Wu, N., Wang, Y., Fang, X., et al., 2013a. The impacts of climate change and human activities on biogeochemical cycles on the Qinghai-Tibetan Plateau. Glob. Chang. Biol. 19, 2940–2955. https://doi.org/10.1111/gcb.12277.

Chen, H., Zhu, Qa, Peng, C., Wu, N., Wang, Y., Fang, X., et al., 2013b. Methane emissions from rice paddies natural wetlands, lakes in China: synthesis new estimate. Glob. Chang. Biol. 19, 19–32.

Collins, W., Bellouin, N., Doutriaux-Boucher, M., Gedney, N., Hinton, T., Jones, C., et al., 2008. Evaluation of the HadGEM2 model. Hadley Cent. Tech. Note. 74.

Cramer, W., Kicklighter, D., Bondeau, A., Iii, B.M., Churkina, G., Nemry, B., et al., 1999. Comparing global models of terrestrial net primary productivity (NPP): overview and key results. Glob. Chang. Biol. 5, 1–15.

Cui, M., Ma, A., Qi, H., Zhuang, X., Zhuang, G., Zhao, G., 2015. Warmer temperature accelerates methane emissions from the Zoige wetland on the Tibetan Plateau without changing methanogenic community composition. Sci. Rep. 5, 11616. https://doi.org/10.1038/srep11616.

Dean, J.F., Middelburg, J.J., Röckmann, T., Aerts, R., Blauw, L.G., Egger, M., et al., 2018. Methane feedbacks to the global climate system in a warmer world. Rev. Geophys. 56, 207–250. https://doi.org/10.1002/2017RG000559.

Ding, W., Cai, Z., Tsuruta, H., Li, X., 2002. Effect of standing water depth on methane emissions from freshwater marshes in northeast China. Atmos. Environ. 36, 5149–5157.

Ding, W., Cai, Z., Wang, D., 2004. Preliminary budget of methane emissions from natural wetlands in China. Atmos. Environ. 38, 751–759.

Dorodnikov, M., Knorr, K., Kuzyakov, Y., Wilmking, M., 2011. Plant-mediated CH_4 transport and contribution of photosynthates to methanogenesis at a boreal mire: a 14C pulse-labeling study. Biogeosciences 8, 2365–2375. https://doi.org/10.5194/bg-8-2365-2011.

Editorial Committee, 2009. China Wetlands Encyclopedia. Beijing Science and Technology Press (in Chinese, 706 pp.).

Erwin, K.L., 2009. Wetlands and global climate change: the role of wetland restoration in a changing world. Wetl. Ecol. Manag. 17, 71–84.

FAO/IIASA/ISRIC/ISS-CAS/JRC, 2008. Harmonized World Soil Database, Version 1.0. FAO, Rome, Italy and IIASA, Laxenburg, Austria (42 pp.).

FAO/IIASA/ISRIC/ISS-CAS/JRC, 2012. Harmonized World Soil Database, Version 1.2. FAO and IIASA, Rome, Italy and Laxenburg, Austria (43 pp.).

Feng, S., Tang, M., Wang, D., 1998. New evidence for the Qinghai-Xizang (Tibet) Plateau as a pilot region of climatic fluctuation in China. Chin. Sci. Bull. 43, 1745–1749.

Frenzel, P., Karofeld, E., 2000. CH_4 emission from a hollow-ridge complex in a raised bog: the role of CH4 production and oxidation. Biogeochemistry 51, 91–112.

Fung, I., John, J., Lerner, J., Matthews, E., Prather, M., Steele, L., et al., 1991. Three-dimensional model synthesis of the global methane cycle. J. Geophys. Res. 96 (D7), 13033–13065. https://doi.org/10.1029/91JD01247.

Gao, Q., Guo, Y., Xu, H., Ganjurjav, H., Li, Y., Wan, Y., et al., 2016. Climate change and its impacts on vegetation distribution and net primary productivity of the alpine ecosystem in the Qinghai-Tibetan Plateau. Sci. Total Environ. 554–555, 34–41.

Giorgetta, M.A., Jungclaus, J., Reick, C.H., Legutke, S., Bader, J., Böttinger, M., et al., 2013. Climate and carbon cycle changes from 1850 to 2100 in MPI-ESM simulations for the Coupled Model Intercomparison Project phase 5. J. Adv. Model. Earth Syst. 5, 572–597.

Gomez-Casanovas, N., Hudiburg, T.W., Bernacchi, C.J., Parton, W.J., DeLucia, E.H., 2016. Nitrogen deposition and greenhouse gas emissions from grasslands: uncertainties and future directions. Glob. Chang. Biol. 22, 1348–1360. https://doi.org/10.1111/gcb.13187.

Hirota, M., Tang, Y., Hu, Q., Hirata, S., Kato, T., Mo, W., et al., 2004. Methane emissions from different vegetation zones in a Qinghai-Tibetan Plateau wetland. Soil Biol. Biochem. 36, 737–748.

Hodson, E., Poulter, B., Zimmermann, N., Prigent, C., Kaplan, J.O., 2011. The El Niño–Southern Oscillation and wetland methane interannual variability. Geophys. Res. Lett. 38, L08810. https://doi.org/10.1029/2011GL046861.

Hu, S., Niu, Z., HaiYing, Z., YanFen, C., Ning, G., 2015. Simulation of spatial distribution of China potential wetland. Chin. Sci. Bull. 60. https://doi.org/10.1360/N972015-00358.

Hu, S., Niu, Z., Chen, Y., Li, L., Zhang, H., 2017. Global wetlands: potential distribution, wetland loss, and status. Sci. Total Environ. 586, 319–327.

Huang, Y., Sass, R.L., Fisher, F.M., 1998a. Model estimates of methane emission from irrigated rice cultivation of China. Glob. Chang. Biol. 4, 809–821.

Huang, Y., Sass, R.L., Fisher Jr., F.M., 1998b. A semi-empirical model of methane emission from flooded rice paddy soils. Glob. Chang. Biol. 4, 247–268.

Huang, Y., Zhang, W., Zheng, X., Li, J., Yu, Y., 2004. Modeling methane emission from rice paddies with various agricultural practices. J. Geophys. Res.-Atmos. 109 (1984–2012).

IPCC, 2013. Climate change 2013: the physical science basis. Contribution of Working Group I to the Fifth Assessment Report of the Intergovernmental Panel on Climate Change. Cambridge University Press, Cambridge.

Ji, Z., Kang, S., 2013. Double-nested dynamical downscaling experiments over the Tibetan Plateau and their projection of climate change under two RCP scenarios. J. Atmos. Sci. 70, 1278–1290.

Jin, H., Wu, J., Cheng, G., Nakano, T., Sun, G., 1999. Methane emissions from wetlands on the Qinghai-Tibet Plateau. Chin. Sci. Bull. 44, 2282–2286.

Jin, Z., Zhuang, Q., He, J.-S., Zhu, X., Song, W., 2015. Net exchanges of methane and carbon dioxide on the Qinghai-Tibetan Plateau from 1979 to 2100. Environ. Res. Lett. 10, 085007.

Joabsson, A., Christensen, T.R., 2001. Methane emissions from wetlands and their relationship with vascular plants: an Arctic example. Glob. Chang. Biol. 7, 919–932.

Joabsson, A., Christensen, T.R., Wallén, B., 1999. Influence of Vascular Plant Photosynthetic Rate on CH 4 Emission From Peat Monoliths From Southern Boreal Sweden. vol. 18. Blackwell Synergy, pp. 215–220.

King, J.Y., Reeburgh, W.S., 2002. A pulse-labeling experiment to determine the contribution of recent plant photosynthates to net methane emission in arctic wet sedge tundra. Soil Biol. Biochem. 34, 173–180.

Kip, N., van Winden, J.F., Pan, Y., Bodrossy, L., Reichart, G.-J., Smolders, A.J., et al., 2010. Global prevalence of methane oxidation by symbiotic bacteria in peat-moss ecosystems. Nat. Geosci. 3, 617–621.

Kleinen, T., Brovkin, V., Schuldt, R., 2012. A dynamic model of wetland extent and peat accumulation: results for the Holocene. Biogeosciences 9, 235–248.

Lanza, L., Ramirez, J., Todini, E., 2001. Stochastic rainfall interpolation and downscaling. Hydrol. Earth Syst. Sci. Discuss. 5, 139–143.

Lew, S., Glińska-Lewczuk, K., 2018. Environmental controls on the abundance of methanotrophs and methanogens in peat bog lakes. Sci. Total Environ. 645, 1201–1211. https://doi.org/10.1016/j.scitotenv.2018.07.141.

Li, L., Yang, S., Wang, Z., Zhu, X., Tang, H., 2010a. Evidence of warming and wetting climate over the Qinghai-Tibet Plateau. Arct. Antarct. Alp. Res. 42, 449–457.

Li, T., Huang, Y., Zhang, W., Song, C., 2010b. $CH4MOD_{wetland}$: a biogeophysical model for simulating methane emissions from natural wetlands. Ecol. Model. 221, 666–680.

Li, T., Huang, Y., Zhang, W., Yu, Y.-Q., 2012. Methane emissions associated with the conversion of marshland to cropland and climate change on the Sanjiang Plain of northeast China from 1950 to 2100. Biogeosciences 9, 5199–5215.

Li, L., Lin, P., Yu, Y., Wang, B., Zhou, T., Liu, L., et al., 2013. The flexible global ocean-atmosphere-land system model, Grid-point Version 2: FGOALS-g2. Adv. Atmos. Sci. 30, 543–560.

Li, T., Zhang, W., Zhang, Q., Lu, Y., Wang, G., Niu, Z., et al., 2015. Impacts of climate and reclamation on temporal variations in CH_4 emissions from different wetlands in China: from 1950 to 2010. Biogeosciences 12, 6853–6868. https://doi.org/10.5194/bg-12-6853-2015.

Li, T., Raivonen, M., Alekseychik, P., Aurela, M., Lohila, A., Zheng, X., et al., 2016a. Importance of vegetation classes in modeling CH4 emissions from boreal and subarctic wetlands in Finland. Sci. Total Environ. 572, 1111–1122.

Li, T., Zhang, Q., Cheng, Z., Ma, Z., Liu, J., Luo, Y., et al., 2016b. Modeling CH_4 emissions from natural wetlands on the Tibetan Plateau over the past 60 years: influence of climate change and wetland loss. Atmosphere 7 (7), 90. https://doi.org/10.3390/atmos7070090.

Li, T., Zhang, Q., Zhang, W., Wang, G., Lu, Y., Yu, L., et al., 2016c. Prediction CH4 emissions from the wetlands in the Sanjiang Plain of northeastern China in the 21st century. PLoS One 11 (7), e0158872. https://doi.org/10.1371/journal.pone.0158872.

Li, T., Zhang, Q., Cheng, Z., Wang, G., Yu, L., Zhang, W., 2017. Performance of CH4MOD wetland for the case study of different regions of natural Chinese wetland. J. Environ. Sci. 57, 356–369.

Liu, L., Greaver, T.L., 2009. A review of nitrogen enrichment effects on three biogenic GHGs: the CO2 sink may be largely offset by stimulated N2O and CH4 emission. Ecol. Lett. 12, 1103–1117.

Liu, X., Yin, Z.Y., 2002. Sensitivity of East Asian monsoon climate to the uplift of the Tibetan Plateau. Palaeogeogr. Palaeoclimatol. Palaeoecol. 183, 223–245.

Liu, J., Zhu, Q., Shen, Y., Yang, Y., Luo, Y., Peng, C., 2015. Spatiotemporal variations of natural wetland CH_4 emissions over China under future climate change. J. Appl. Ecol. 26, 3467–3474 (in Chinese with English abstract).

Lu, X., Zhuang, Q., 2012. Modeling methane emissions from the Alaskan Yukon River basin, 1986–2005, by coupling a large-scale hydrological model and a process-based methane model. J. Geophys. Res. Biogeosci. 117, G02010. https://doi.org/10.1029/2011JG001843.

Marthews, T., Dadson, S., Lehner, B., Abele, S., Gedney, N., 2015. High-resolution global topographic index values for use in large-scale hydrological modelling. Hydrol. Earth Syst. Sci. 19, 91–104.

McGuire, A.D., Melillo, J., Joyce, L., Kicklighter, D., Grace, A., Moore, B., et al., 1992. Interactions between carbon and nitrogen dynamics in estimating net primary productivity for potential vegetation in North America. Glob. Biogeochem. Cycles 6, 101–124.

Melillo, J.M., McGuire, A.D., Kicklighter, D.W., Moore, B., Vorosmarty, C.J., Schloss, A.L., 1993. Global climate change and terrestrial net primary production. Nature 363, 234–240.

Melton, J., Wania, R., Hodson, E., Poulter, B., Ringeval, B., Spahni, R., et al., 2013. Present state of global wetland extent and wetland methane modelling: conclusions from a model intercomparison project (WETCHIMP). Biogeosciences 10, 753–788. https://doi.org/10.5194/bg-10-753-2013.

Minoda, T., Kimura, M., Wada, E., 1996. Photosynthates as dominant source of CH4 and CO2 in soil water and CH_4 emitted to the atmosphere from paddy fields. J. Geophys. Res.-Atmos. 101, 21091–21097.

Mitsch, W.J., Gosselink, J.G., 2007. Wetlands. John Wiley & Sons, Inc., Hoboken.

Moore, T.R., Roulet, N.T., 1993. Methane flux: water table relations in northern wetlands. Geophys. Res. Lett. 20, 587–590.

Myhre, G., Shindell, D., Bréon, F.-M., Collins, W., Fuglestvedt, J., Huang, J., et al., 2013. Anthropogenic and natural radiative forcing. Climate Change 423, 658–740.

Niu, Z., Zhang, H., Wang, X., Yao, W., Zhou, D., Zhao, K., et al., 2012. Mapping wetland changes in China between 1978 and 2008. Chin. Sci. Bull. 57, 2813–2823 (in Chinese with English abstract).
Papa, F., Prigent, C., Aires, F., Jimenez, C., Rossow, W.B., Matthews, E., 2010. Interannual variability of surface water extent at the global scale, 1993–2004. J. Geophys. Res.-Atmos. 115, D12111. https://doi.org/10.1029/2009JD012674.
Poindexter, C.M., Baldocchi, D.D., Matthes, J.H., Knox, S.H., Variano, E.A., 2016. The contribution of an overlooked transport process to a wetland's methane emissions. Geophys. Res. Lett. 43, 6276–6284.
Schipper, L.A., Hobbs, J.K., Rutledge, S., Arcus, V.L., 2014. Thermodynamic theory explains the temperature optima of soil microbial processes and high Q10 values at low temperatures. Glob. Chang. Biol. 20, 3578–3586. https://doi.org/10.1111/gcb.12596.
Schwalb, A., Steeb, P., Wrozyna, C., Mäusbacher, R., Daut, G., Wallner, J., et al., 2008. The top of the world as a climate sensor. Ger. Res. 30, 4–7.
Serrano-Silva, N., Sarria-Guzmán, Y., Dendooven, L., Luna-Guido, M., 2014. Methanogenesis and methanotrophy in soil: a review. Pedosphere 24, 291–307.
Shindell, D.T., Walter, B.P., Faluvegi, G., 2004. Impacts of climate change on methane emissions from wetlands. Geophys. Res. Lett. 31, L21202. https://doi.org/10.1029/2004GL021009.
Shindell, D.T., Faluvegi, G., Koch, D.M., Schmidt, G.A., Unger, N., Bauer, S.E., 2009. Improved attribution of climate forcing to emissions. Science 326, 716–718.
Song, W., Wang, H., Wang, G., Chen, L., Jin, Z., Zhuang, Q., et al., 2015. Methane emissions from an alpine wetland on the Tibetan Plateau: neglected but vital contribution of the nongrowing season. J. Geophys. Res. Biogeosci. 120, 1475–1490.
Song, Y., Jin, L., Wang, H., 2018. Vegetation changes along the Qinghai-Tibet Plateau engineering corridor since 2000 induced by climate change and human activities. Remote Sens. 10, 95. https://doi.org/10.3390/rs10010095.
Ström, L., Mastepanov, M., Christensen, T.R., 2005. Species-specific effects of vascular plants on carbon turnover and methane emissions from wetlands. Biogeochemistry 75, 65–82.
van Winden, J.F., Reichart, G.-J., McNamara, N.P., Benthien, A., Damsté, J.S.S., 2012. Temperature-Induced increase in methane release from peat bogs: A mesocosm experiment. PLoS One 7, e39614.
Walker, T.N., Garnett, M.H., Ward, S.E., Oakley, S., Bardgett, R.D., Ostle, N.J., 2016. Vascular plants promote ancient peatland carbon loss with climate warming. Glob. Chang. Biol. https://doi.org/10.1111/gcb.13213.
Wang, D., Lu, X., Ding, W., Cai, Z., Gao, J., Yang, F., 2002. Methane emission from marshes in Zoige Plateau. Adv. Earth Science 17, 877–880 (in Chinese with English abstract).
Wang, Z., Wu, J., Madden, M., Mao, D., 2012. China's wetlands: conservation plans and policy impacts. Ambio 41, 782–786.
Watanabe, S., Hajima, T., Sudo, K., Nagashima, T., Takemura, T., Okajima, H., et al., 2011. MIROC-ESM 2010: model description and basic results of CMIP5-20c3m experiments. Geosci. Model Dev. 4, 845–872.
Wei, D., Wang, X., 2016. CH_4 exchanges of the natural ecosystems in China during the past three decades: the role of wetland extent and its dynamics. J. Geophys. Res. Biogeosci. 121, 2445–2463.
Wei, D., Wang, X., 2017. Recent climatic changes and wetland expansion turned Tibet into a net CH_4 source. Clim. Chang. 144, 657–670.
Wei, D., Tarchen, T., Dai, D., Wang, Y., Wang, Y., 2015. Revisiting the role of CH_4 emissions from alpine wetlands on the Tibetan Plateau: evidence from two in situ measurements at 4758 and 4320 m above sea level. J. Geophys. Res. Biogeosci. 120, 1741–1750.
Whalen, S.C., 2005. Biogeochemistry of methane exchange between natural wetlands and the atmosphere. Environ. Eng. Sci. 22, 73–94.
Whiting, G.J., Chanton, J.P., 1992. Plant-dependent CH_4 emission in a subarctic Canadian fen. Glob. Biogeochem. Cycles 6, 225–231.
Whiting, G.J., Chanton, J.P., 1993. Primary production control of methane emission from wetlands. Nature 364, 794–795.
Wieder, W.R., Cleveland, C.C., Smith, W.K., Todd-Brown, K., 2015. Future productivity and carbon storage limited by terrestrial nutrient availability. Nat. Geosci. 8, 441–444.
Xu, X., Tian, H., 2012. Methane exchange between marshland and the atmosphere over China during 1949–2008. Glob. Biogeochem. Cycles 26, GB2006. https://doi.org/10.1029/2010GB003946.
Xue, Z., Zhang, Z., Lu, X., Zou, Y., Lu, Y., Jiang, M., et al., 2014. Predicted areas of potential distributions of alpine wetlands under different scenarios in the Qinghai-Tibetan Plateau, China. Glob. Planet. Chang. 123, 77–85.
Yao, T., Pu, J., Lu, A., Wang, Y., Yu, W., 2007. Recent glacial retreat and its impact on hydrological processes on the Tibetan Plateau, China, and surrounding regions. Arct. Antarct. Alp. Res. 39, 642–650.
Yvon-Durocher, G., Allen, A.P., Bastviken, D., Conrad, R., Gudasz, C., St-Pierre, A., et al., 2014. Methane fluxes show consistent temperature dependence across microbial to ecosystem scales. Nature 507, 488–491. https://doi.org/10.1038/nature13164.
Zhang, X., Jiang, H., 2014. Spatial variations in methane emissions from natural wetlands in China. Int. J. Environ. Sci. Technol. 11, 77–86.
Zhang, Y., Wang, G., Wang, Y., 2011. Changes in alpine wetland ecosystems of the Qinghai–Tibetan plateau from 1967 to 2004. Environ. Monit. Assess. 180, 189–199.
Zhang, R., Su, F., Jiang, Z., Gao, X., Guo, D., Ni, J., et al., 2015. An overview of projected climate and environmental changes across the Tibetan Plateau in the 21st century. Chin. Sci. Bull. 60, 3036–3047. https://doi.org/10.1360/N972014-01296 (in Chinese with English abstract).
Zhang, Z., Zimmermann, N.E., Kaplan, J.O., Poulter, B., 2016. Modeling spatiotemporal dynamics of global wetlands: comprehensive evaluation of a new sub-grid TOPMODEL parameterization and uncertainties. Biogeosciences 13, 1387–1408.
Zhang, Z., Zimmermann, N.E., Stenke, A., Li, X., Hodson, E.L., Zhu, G., et al., 2017. Emerging role of wetland methane emissions in driving 21st century climate change. Proc. Natl. Acad. Sci. 114 (36), 9647–9652.
Zhao, L., Ping, C.L., Yang, D., Cheng, G., Ding, Y., Liu, S., 2004. Changes of climate and seasonally frozen ground over the past 30 years in Qinghai–Xizang (Tibetan) Plateau, China. Glob. Planet. Chang. 43, 19–31.
Zheng, Y., Niu, Z., Gong, P., Dai, Y., Shangguan, W., 2013. Preliminary estimation of the organic carbon pool in China's wetlands. Chin. Sci. Bull. 58, 662–670. https://doi.org/10.1007/s11434-012-5529-9 (in Chinese with English abstract).
Zhou, L., Hélène, G., Yujie, H., Qianlai, Z., David, M.A., Alec, B., et al., 2018. The role of environmental driving factors in historical and projected carbon dynamics of wetland ecosystems in Alaska. Ecol. Appl. 0, 1–19.
Zhu, X., Zhuang, Q., Gao, X., Sokolov, A., Schlosser, C.A., 2013. Pan-Arctic land-atmospheric fluxes of methane and carbon dioxide in response to climate change over the 21st century. Environ. Res. Lett. 8, 045003. https://doi.org/10.1088/1748-9326/8/4/045003.
Zhu, Q., Peng, C., Liu, J., Jiang, H., Fang, X., Chen, H., et al., 2016. Climate-driven increase of natural wetland methane emissions offset by human-induced wetland reduction in China over the past three decades. Sci. Rep. 6, 38020. https://doi.org/10.1038/srep38020.
Zhuang, Q., Melillo, J.M., Kicklighter, D.W., Prinn, R.G., McGuire, A.D., Steudler, P.A., et al., 2004. Methane fluxes between terrestrial ecosystems and the atmosphere at northern high latitudes during the past century: a retrospective analysis with a process-based biogeochemistry model. Glob. Biogeochem. Cycles 18, GB3010. https://doi.org/10.1029/2004GB002239.
Zhuang, Q., Melillo, J.M., Sarofim, M.C., Kicklighter, D.W., McGuire, A.D., Felzer, B.S., et al., 2006. CO_2 and CH_4 exchanges between land ecosystems and the atmosphere in northern high latitudes over the 21st century. Geophys. Res. Lett. 33, L17403. https://doi.org/10.1029/2006GL026972.
Zhuang, Q., He, J., Lu, Y., Ji, L., Xiao, J., Luo, T., 2010. Carbon dynamics of terrestrial ecosystems on the Tibetan Plateau during the 20th century: an analysis with a process-based biogeochemical model. Glob. Ecol. Biogeogr. 19, 649–662.